References

AALST, W. VAN, DEN HOLLANDER, J., PETERSE, W. J. A. M. & DE WOLFF, P. M. (1976). *Acta Cryst.* B**32**, 47–58.

B. A. FRENZ & ASSOCIATES INC. (1982). *SDP Structure Determination Package*. College Station, Texas, USA.

BLOWER, S. K. & GREAVES, C. (1988). *Acta Cryst.* C**44**, 587–589.

CAVA, R. J., SIEGRIST, T., HESSEN, B., KRAJEWSKI, J. J., PECK, W. F., BATLOGG, B. JR, TAKAGI, H., WASZCZAK, J. V., SCHNEEMEYER, L. E. & ZANDBERGEN H. W. (1991). *J. Solid State Chem.* **94**, 170–184.

DOUDIN, B. (1985). Private communication.

ER-RAKHO, L., MICHEL, C. & RAVEAU, B. (1988). *J. Solid State Chem.* **73**, 514–519.

GAO, Y., LEE, P., YE, J., BUSH, P., PETRICEK, V. & COPPENS, P. (1989). *Physica C*, **160**, 431–438.

IMAI, K., NAKAI, I., KAWASHIMA, T., SUENO, S. & ONO, A. (1988). *Jpn. J. Appl. Phys.* **27**, 1661–1664.

LIGHTFOOT, P., HRILJAC, J. A., PEI, S., ZHENG, Y., MITCHELL, A. W., RICHARDS, D. R., DABROWSKI, B., JORGENSEN, J. D. & HINKS, D. G. (1991). *J. Solid State Chem.* **92**, 473–479.

MATSUI, Y., TAKEKAWA, S., HORIUCHI, S. & UMEZONO, A. (1988). *Jpn. J. Appl. Phys.* **27**, 1873–1876.

MICHEL, C., HERVIEU, M., BOREL, M. M., GRANDIN, A., DESLANDES, F., PROVOST, J. & RAVEAU, B. (1987). *Z. Phys. Condens. Matter*, B**68**, 421–423.

ONODA, M. & SATO, M. (1988). *Solid State Commun.* **67**, 799–804.

SHANNON, R. D. (1976). *Acta Cryst.* A**32**, 751–767.

TARASCON, J. M., LE PAGE, Y. & MCKINNON, W. R. (1990). *Eur. J. Solid State Inorg. Chem.* **27**, 81–104.

TARASCON, J. M., LE PAGE, Y., MCKINNON, W. R., RAMESH, R., EIBSCHUTZ, M., TSELEPIS, E., WANG, E. & HULL, G. W. (1990). *Physica C*, **167**, 20–34.

TARASCON, J. M., MICELI, P. F., BARBOUX, P., HWANG, D. M., HULL, G. W., GIROUD, M., GREENE, L. H. LE PAGE, Y., MCKINNON, W. R., TSELEPIS, E., PLEIZIER, G., EIBSCHUTZ, M., NEUMANN, D. A. & RHYNE, J. J. (1989). *Phys. Rev. B*, **39**, 11587–11598.

TORARDI, C. C., PARISE, J. B., SANTORO, A., RAWN, C. J., ROTH, R. S. & BURTON, B. P. (1991). *J. Solid State Chem.* **93**, 228–235.

TORARDI, C. C., SUBRAMANIAN, M. A., CALABRESE, J. C., GOPALAKRISHNAN, J., MCCARRON, E. M., MORRISSEY, K. J., ASKEW, T. R., FLIPPEN, R. B., CHOWDHRY, U. & SLEIGHT, A. W. (1988). *Phys. Rev. B*, **38**, 225–231.

VON SCHNERING, H. G., WALZ, L., SCHWARZ, M., BECKER, W., HARTWEG, M., POPP, T., HETTICH, B., MÜLLER, P. & KÄMPF, G. (1988). *Angew. Chem. Int. Ed. Engl.* **27**, 574–576.

WOLFF, P. M. DE (1977). *Acta Cryst.* A**33**, 493–497.

WOLFF, P. M. DE, JANSSEN, T. & JANNER, A. (1981). *Acta Cryst.* A**37**, 625–636.

YAMAMOTO, A. (1982). *REMOS*. A computer program for the refinement of modulated structures. National Institute for Research in Inorganic Materials, Niiharigun, Ibaraki, Japan.

YAMAMOTO, A., NAKAZAWA, H., KITAMURA, M. & MORIMOTO, N. (1984). *Acta Cryst.* B**40**, 228–237.

YAMAMOTO, A., ONODA, M., TAKAYAMA-MUROMACHI, E., IZUMI, F., ISHIGAKI, T. & ASANO, H. (1990). *Phys. Rev. B*, **42**, 4228–4239.

ZUÑIGA, F. J., MADARIAGA, G., PACIOREK, W. A., PÉREZ-MATO, J. M., EZPELETA, J. M. & ETXEBARRIA, I. (1989). *Acta Cryst.* B**45**, 566–576.

Acta Cryst. (1992). B**48**, 418–428

Structure Refinement of Commensurately Modulated Bismuth Strontium Tantalate, $Bi_2SrTa_2O_9$

BY A. DAVID RAE

School of Chemistry, University of New South Wales, PO Box 1, Kensington, New South Wales 2033, Australia

AND JOHN G. THOMPSON AND RAY L. WITHERS

Research School of Chemistry, Australian National University, GPO Box 4, Canberra, ACT 2601, Australia

(*Received* 6 *November* 1991; *accepted* 4 *February* 1992)

Abstract

The displacive ferroelectric $Bi_2SrTa_2O_9$ [M_r = 1011.47, a = 5.5306 (5), b = 5.5344 (5), c = 24.9839 (24) Å, Z = 4, D_x = 8.785 g cm^{-3}, Mo $K\alpha$, λ = 0.7107 Å, μ = 806.8 cm^{-1}, $F(000)$ = 1687.64], is described at room temperature in space group $A2_1am$ as a commensurate modulation of an idealized $Fmmm$ parent structure derived from an $I4/mmm$ structure. A final value of 0.045 for $R_1 = \sum_{\mathbf{h}}||F_{obs}(\mathbf{h})| - |F_{calc}(\mathbf{h})||/\sum_{\mathbf{h}}|F_{obs}(\mathbf{h})|$ was obtained for 3082 unmerged data with $I(\mathbf{h}) > 3\sigma[I(\mathbf{h})]$. The crystal studied showed both twinning and disorder which were successfully modelled in the refinement. The final structure suggests that these features are almost inevitable. The structure is contrasted with that of Bi_3TiNbO_9 [Thompson, Rae, Withers & Craig (1991), *Acta Cryst.* B**47**, 174–180] with particular interest in the effects of a Bi^{3+} ion being replaced by an Sr^{2+} ion. The value of anomalous dispersion for detecting false minima, centrosymmetric twinning and disorder is detailed. An apparent valence interpretation of the crystal chemistry is included.

Introduction

In recent years the room-temperature crystal structures of the ferroelectric Aurivillius phases,

0108-7681/92/040418-11$06.00

$Bi_4Ti_3O_{12}$ (Rae, Thompson, Withers & Willis, 1990), Bi_3TiNbO_9 (Thompson, Rae, Withers & Craig, 1991) and Bi_2WO_6 (Rae, Thompson & Withers, 1991) have been re-refined from single-crystal X-ray diffraction data using a modulated structure approach. Their room-temperature structures can be described in terms of relatively small amplitude, displacive pertubations from a high-symmetry parent structure (space-group symmetry $I4/mmm$, $\mathbf{a}_p = \mathbf{b}_p \simeq 3.85$ Å, p = perovskite).

In all of the Aurivillius phases we have studied we have regarded the resulting space groups as having been derived from a parent structure of *Fmmm* symmetry. Since this *Fmmm* structure may itself be described as a derivative of a structure of $I4/mmm$ symmetry it has been customary to define **c** as the long axis and to select **a** as the polar axis direction for ferroelectricity. In order to simplify the modulated-structure approach we have selected symmetry operations of the standard setting of *Fmmm* and have not redefined the origin or orientation to coincide with standard settings of *International Tables for X-ray Crystallography* (1974, Vol. IV).

From the experience obtained from the above three structure re-refinements we can make several general observations:

(1) The refinements of crystal structures involving small perturbations away from a high-symmetry parent structure are strongly susceptible to false refinement minima in certain circumstances. These circumstances can be recognized using a modulated-structure approach to refinement. The earlier refinements of $Bi_4Ti_3O_{12}$ (Dorrian, Newnham, Smith & Kay, 1971), Bi_3TiNbO_9 (Wolfe, Newnham, Smith & Kay, 1971) and Bi_2WO_6 (Wolfe, Newnham & Kay, 1969) all suffered from false minima.

(2) When using single-crystal X-ray diffraction data from such strongly absorbing materials (μ = 700–1000 cm^{-1} for Mo $K\alpha$) the best possible correction for absorption is essential if the data is to be of sufficient quality to discriminate between true and false refinement minima. When crystals can be grown as thin plates, the thickness of the plate can be refined to an accuracy of about 1–3% using data correlation. (Exclusion of low-angle intense data that is extinction affected is recommended.) Mounting the crystal so the normal to the plate is approximately in the horizontal plane of the diffractometer restricts the number of reflections with large absorption corrections. However correlations between these high-absorption reflections with less-absorbed equivalents are very susceptible to plate thickness. The high-absorption data can be excluded from the refinement yet still be monitored to assess the quality of the absorption correction.

(3) While the presence of the very heavy atom Bi in these structures exacerbates the absorption problem for X-rays it actually helps, by virtue of its large anomalous dispersion ($\Delta f'' = 10.599$) for Mo $K\alpha$ (*International Tables for X-ray Crystallography*, 1974, Vol. IV), to resolve by comparative refinement the otherwise intractable problem of pseudo-homometric solutions. This resolution is a consequence of the anomalous dispersion creating a correlation between the phases of symmetrized components of the scattering density that otherwise would make uncorrelated contributions to the intensity. This advantage is lost in neutron diffraction refinements.

(4) As the perturbations from the parent structure are of relatively small amplitude the 'as synthesized' crystals are not necessarily ordered single crystals and often show evidence of this departure from the ideal which can and should be included in the refinement model. Partial twinning was a feature of $Bi_4Ti_3O_{12}$ (Rae *et al.*, 1990) and coherently intergrown modulated variants were a feature of Bi_2WO_6 (Rae *et al.*, 1991). In both these structures the average structure and certain of the modulation modes were coherent across the twin or intergrowth boundaries.

It is also possible to make observations concerning the crystal chemistry of the underlying ferroelectricity in the Aurivillius phases using the concept of bond valence (Brown, 1978, 1981). While these have been discussed at length elsewhere (Withers, Thompson & Rae, 1991) the key features are:

(1) The bond-valence sums or apparent valences (AV's) for the O atoms bonded to the Bi atoms in the Bi_2O_2 layer are significantly higher than two on one side and lower than two on the other side of the Bi atom which has a stereoactive lone pair of electrons. This feature appears to indicate satisfactory bonding.

(2) The large spontaneous polarizations observed along **a** can be largely attributed to the gross underbonding of Bi^{3+} in the perovskite A site, and to a lesser extent the underbonding of Bi^{3+} in the Bi_2O_2 layer, in the parent structure. In the case of Bi_2WO_6 the first cause is absent as there is no perovskite A site.

(3) The concerted rotations of corner-connected octahedra about the **a** and **c** axes serve to alleviate the overbonding of the perovskite B atom in the parent structure.

(4) The calculation of AV's for refined structural models provides a clear indication as to whether the model is chemically plausible, and often helps distinguish between structure solutions which cannot easily be discriminated solely from refinement statistics.

The crystal structure of $(Sr_{0.9}Ba_{0.1})Bi_2Ta_2O_9$ (Newnham, Wolfe, Horsey, Diaz-Colon & Kay, 1973) was of particular interest because it represents

an Aurivillius phase which does not contain Bi^{3+} in the perovskite *A* site. To be consistent with the second point above, the spontaneous polarization has to be substantially less than the isostructural Bi_3TiNbO_9 and indeed this was the case. However, the reported structure displayed rather unlikely AV's, even taking into account the anomaly mentioned in the first point above. As discussed previously (Withers *et al.*, 1991) displacive perturbations from a high-symmetry parent structure will always increase the AV for the perovskite *A* site. This is desirable for a 3^+ ion at this site but for a 2^+ ion such as $(Sr_{0.9}Ba_{0.1})$ in the $(Sr_{0.9}Ba_{0.1})Bi_2Ta_2O_9$ structure the 2^+ ion is already overbonded in the parent structure. This creates a problem that the correct structure solution must resolve, albeit by compromise. The published structure was refined using both single-crystal X-ray and neutron powder diffraction data but the final R_1 factor was only 0.13.

The refinements of $Bi_4Ti_3O_{12}$ (Dorrian *et al.*, 1971), Bi_3TiNbO_9 (Wolfe *et al.*, 1971) and Bi_2WO_6 (Wolfe *et al.*, 1969) all suffered from the refinement problems mentioned above and it is reasonable to assume that there are errors in the reported structure of $(Sr_{0.9}Ba_{0.1})Bi_2Ta_2O_9$. In order to simplify both the refinement of a structure with a 2^+ ion in the perovskite *A* site and subsequent discussion in terms of bond valences we chose to study $Bi_2SrTa_2O_9$ (see Fig. 1) based on the earlier observations that only the Curie temperature T_c showed any substantial sensitivity to replacing Sr by Ba. The structure obtained was compatible with AV concepts and proved to be a good test of the application of the bond-valence concept to displacive ferroelectrics.

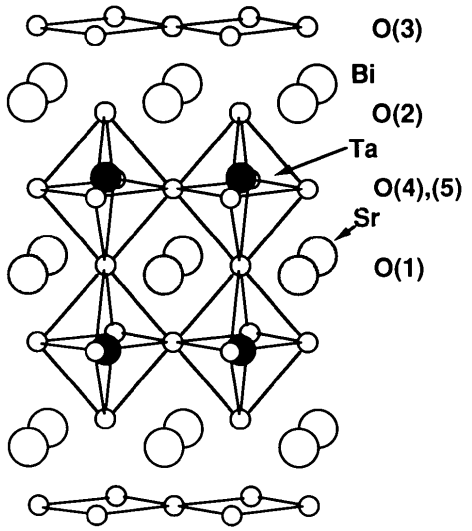

Fig. 1. A perspective drawing, approximately down ⟨110⟩, of the undistorted *Fmmm* parent structure of $Bi_2SrTa_2O_9$. Only atoms between $\frac{1}{4}c$ and $\frac{3}{4}c$ are shown.

Experimental

$Bi_2SrTa_2O_9$ was prepared by solid-state reaction of a mixture of Bi_2O_3 (Atomergic, 99.999%), $SrCO_3$ (Cerac, 99.999%) and Ta_2O_5 (Koch-Light, 99.9%) with mole ratio 1:1:1 at 1473 K in a Pt crucible. Single crystals were grown in a similar manner to that used by Newnham *et al.* (1973) by adding excess Bi_2O_3 as a flux. Slowly cooling this mixture from 1473 to 1173 K over 3 days produced suitable platy crystals at the surface of the two-phase mixture.

Unlike the previous Aurivillius phases which we have studied this material did not display 90° domain walls, so it was necessary to identify twin-free crystals from their X-ray diffraction photographs using a Buerger precession camera. While some crystals appeared to be free of {110} twinning from their precession photographs subsequent examination on the diffractometer showed that all crystals possessed at least a few percent of the other twin. Despite the fact that working with a twinned crystal added an extra degree of freedom to the refinement this was refineable. The crystal chosen for data collection approximated a rectangular plate with the following faces measured from an internal origin: (001) 0.0070, (00$\bar{1}$) 0.0070, (8$\bar{9}$0) 0.061, ($\bar{1}$10) 0.065, (110) 0.084, ($\bar{1}\bar{1}$0) 0.101 mm. Precise measurements of faces were made using the method devised by Alcock (1970). Data correlation of equivalent reflections was used to optimize the thin dimension.

A full sphere of *A*-centred Mo $K\alpha$ monochromated data with $1.5 < \theta < 30°$ was collected using a Picker FACS-I automatic four-circle diffractometer in $\theta/2\theta$ scan mode at 2.0° min^{-1} for a 2θ scan width of $(2.0 + 0.692\tan\theta)°$ with backgrounds of 10 s per side. The numerical absorption correction of *XTAL*3.0 (Hall & Stewart, 1990) used a 14 × 14 × 14 grid with grid layers perpendicular to **c***. The linear absorption coefficient μ(Mo $K\alpha$) was 806.8 cm^{-1} [941 cm^{-1} was used by Newnham *et al.* (1973)]. The unit-cell dimensions were refined from 25 high-angle reflections centred on the $K\alpha_1$ peaks. Scattering curves, atomic absorption corrections and anomalous-dispersion corrections were taken from *International Tables for X-ray Crystallography* (1974, Vol. IV). Values of $wR = [\sum_h N_h \sum_i w_{hi}(|F(\mathbf{h}_i)| - |F(\mathbf{h})|)^2 / \sum_h (N_h - 1)\sum_i w_{hi}|F(\mathbf{h})|^2]^{1/2}$, where N_h is the number of independent observations of $|F(\mathbf{h})|^2$, were obtained using *SHELX* (Sheldrick, 1976) and gave the following results for the merging of data for different assumed symmetries. We note that the statistic for *m*11 is not significantly worse.

Data used	No. of data	*wR* (merge) *m*11	1*m*1	11*m*
All reflections (uncorrected)	4250	0.2333	0.2339	0.0604
All reflections (corrected)	4250	0.0378	0.0390	0.0331
Minus data through fibre	3540	0.0378	0.0385	0.0284
Minus large $\bar{T}$ data	2890	0.0265	0.0407	0.0232

Selection of data

Data were not merged since anisotropic extinction corrections were applied. A 3% error in $F(\mathbf{h})$ was an arbitrary addition to the counting-statistic error in order to match the goodness of fit in different data classes. Refinement excluded data that could have been affected by X-rays passing through the fibre mounting the crystal and used the 3083 data with $I(I\mathbf{h}) > 3\sigma[I(\mathbf{h})]$ from the 3540 remaining data. The 457 truly weak data were monitored and gave a final goodness of fit of 1.11. The $3\sigma[I(\mathbf{h})]$ cutoff for weak data was chosen from inspection of equivalent reflections. Below this cutoff, values of $|F(\mathbf{h})|$ for equivalent reflections were too inconsistent. The insignificance of this data was demonstrated by repeating the final refinement cycle to include those 303 (of 457) weak data with $|F_{calc}(\mathbf{h})| > \sigma[|F_{obs}(\mathbf{h})|]$. The goodness of fit for the 457 weak data reduced from 1.11 to 1.09 demonstrating the lack of information content in these reflections at this stage of refinement. Data were monitored by segmenting according to index, *viz.* *h*, *k*, *l* odd (*o*) or even (*e*). The observed data consisted of 924 *eee* and 941 *ooo* *F*-centred data, and 647 *eoo* and 571 *oee* *A*-centred data. Final refinement statistics are given in Table 3. A small amount of {110} twinning also existed. Symmetry equivalents of *khl* and $-khl$ reflections of these minor twin components correspond to *hkl* reflections of the major twin component and create overlapped spots for *eee* and *ooo* reflections. The totality of both spots was collected and this was accounted for in the least-squares refinement. However the *eoo* and *oee* data for the {110} twin components appear at *oeo* and *eoo* (*B*-centred) positions in the diffraction pattern of the major twin component. These data were not used in the refinement. It is noted that the relative magnitudes of these data were consistent with the final refinement parameters.

Electron diffraction results

Given the proven ability of electron diffraction to observe weak features of reciprocal space not readily detectable *via* conventional X-ray diffraction procedures, crushed single-crystal fragments from the same $Bi_2SrTa_2O_9$ specimen as the single crystal were studied in order to check the previously reported space-group assignment of $A2_1am$. Figs. 2(*a*), 2(*b*) and 2(*c*) show typical [100], [010] and [001] zone-axis convergent-beam patterns (CBP's). It was found to be rather difficult to obtain clean [010] zone-axis patterns (important as they confirm the *a* glide). Small movement of the probe invariably led to switching between patterns (*a*) and (*b*). We conclude that crushing the sample induces 90° twinning on a very fine scale. While the introduction of fine-scale 90° twinning has not been a problem with previously studied members of the Aurivillius family we attribute it in $Bi_2SrTa_2O_9$ as due to the relatively small magnitude of some of the displacive modes present in the room-temperature structure (discussed below). The three patterns in Fig. 2, taken together, require a space-group symmetry of at least $A1a1$ and are certainly compatible with $A2_1am$ space-group symmetry. As a result of beam damage it was not possible to take high-quality convergent-beam patterns to confirm the mirror plane perpendicular to **c**.

The role of anomalous dispersion in determining twinning and disorder

An essential feature of the single-crystal X-ray refinement was the necessity to model the non-ideality of the crystal in order to reduce the value of R_1 below 0.10. A twinning-disorder model was used and the final structure obtained was consistent with such a model. If $F(\mathbf{h})$ is assigned to the value of the structure factor per unit cell for a perfectly ordered untwinned crystal fragment then we can split the structure factor up into components so that

$$F(\mathbf{h}) = A(\mathbf{h}) + iB(\mathbf{h}) + i[A''(\mathbf{h}) + iB''(\mathbf{h})],$$

where the first two terms arise from the real component of the scattering density and the final two components arise from the imaginary component of the scattering density, *i.e.* that contribution arising from the $i\Delta f''$ component of the atomic scattering factors. As a consequence

$$F(-\mathbf{h}) = A(\mathbf{h}) - iB(\mathbf{h}) + i[A''(\mathbf{h}) - iB''(\mathbf{h})].$$

A modulated-structure approach to the space group $A2_1am$ as detailed by Thompson *et al.* (1991) with our origin setting (see earlier) determines that $A(\mathbf{h}) + iA''(\mathbf{h})$ is the Fourier transform of a scattering-density component of *Fmmm* symmetry and $iB(\mathbf{h}) - B''(\mathbf{h})$ is the Fourier transform of a component of *F2mm* symmetry for *F*-centred (*eee* and *ooo*) data whereas $A(\mathbf{h}) + iA''(\mathbf{h})$ is the Fourier transform of a component of *Abam* symmetry and $iB(\mathbf{h}) - B''(\mathbf{h})$ is the Fourier transform of a component of *Amam* symmetry for *A*-centred (*eoo* and *oee*) data. The sign of the *Fmmm* and *Amam* components selects between alternative origins and polarity is determined by the *F2mm* component. Alternative signs for the *Abam* component create indistinguishable intensities but non-equivalent density maps.

Disorder across a mirror plane perpendicular to **a** at $x = 0$ in space group $A2_1am$ leaves the *Amam* and *Fmmm* components of the scattering density unaltered but reverses the sign of the *F2mm* and *Abam* components. This is equivalent to creating observations $Y(\mathbf{h}) = |(1-a)F(\mathbf{h}) + a(-1)^{h+k}F(-\mathbf{h})|^2$.

Twinning of $Y(\mathbf{h})$ with $Y(-\mathbf{h})$ or its symmetry equivalent creates observations $I(\mathbf{h}) = [(1-b)Y(\mathbf{h}) + bY(-\mathbf{h})]$. Regarding the crystal as being made up of a number of such components we obtain an average intensity of

$$\langle I(\mathbf{h})\rangle = [A(\mathbf{h})^2 + A''(\mathbf{h})^2] + k_1[A''(\mathbf{h})B(\mathbf{h}) - B''(\mathbf{h})A(\mathbf{h})] + k_2[B(\mathbf{h})^2 + B''(\mathbf{h})^2]$$

for F-centred data and

$$\langle I(\mathbf{h})\rangle = [B(\mathbf{h})^2 + B''(\mathbf{h})^2] + k_1[B''(\mathbf{h})A(\mathbf{h}) - A''(\mathbf{h})B(\mathbf{h})] + k_2[A(\mathbf{h})^2 + A''(\mathbf{h})^2]$$

for A-centred data where

$$k_1 = 2\langle(1-2a)(1-2b)\rangle \text{ and } k_2 = \langle(1-2a)^2\rangle. \quad (1)$$

This global modification involves just two variables and for refinement purposes we can neglect the averaging process and say that $k_1 = 2(1-2a) \times (1-2b)$ and $k_2 = (1-2a)^2$ where a and b are refined parameters of the program *RAELS*89 (Rae, 1989) used for the least-squares refinement. $Y(\mathbf{h})$ was evaluated by doubling the size of the atom list compared to an ordered model and imposing the mirror symmetry as strict constraints relating the positional and thermal parameters of disorder-related atoms. This removes the need to define the x coordinate of the origin of the structure provided a is non-zero. The refined occupancy parameter $1-a$ applied to atoms of the first half of the list was coupled to the occupancy parameter a that was used for the remaining atoms.

The twinning was further complicated by the existence of a small fraction of {110} twinning and four (rather than two) twin components were used corresponding to hkl, $-hkl$, khl and $-khl$ with refined abundances $1-b-2c$, b, c, c. The final two abundances were set equal as it was impossible to refine the difference between the two Friedel-equivalent components meaningfully. The A-centered data do not contain the last two components.

In the absence of anomalous dispersion equation (1) becomes

$$\langle I(\mathbf{h})\rangle = A(\mathbf{h})^2 + [(1-2a)B(\mathbf{h})]^2 \text{ for } F\text{-centred data}$$

and

$$\langle I(\mathbf{h})\rangle = B(\mathbf{h})^2 + [(1-2a)A(\mathbf{h})]^2 \text{ for } A\text{-centred data} \quad (2)$$

and all information about twinning disappears as

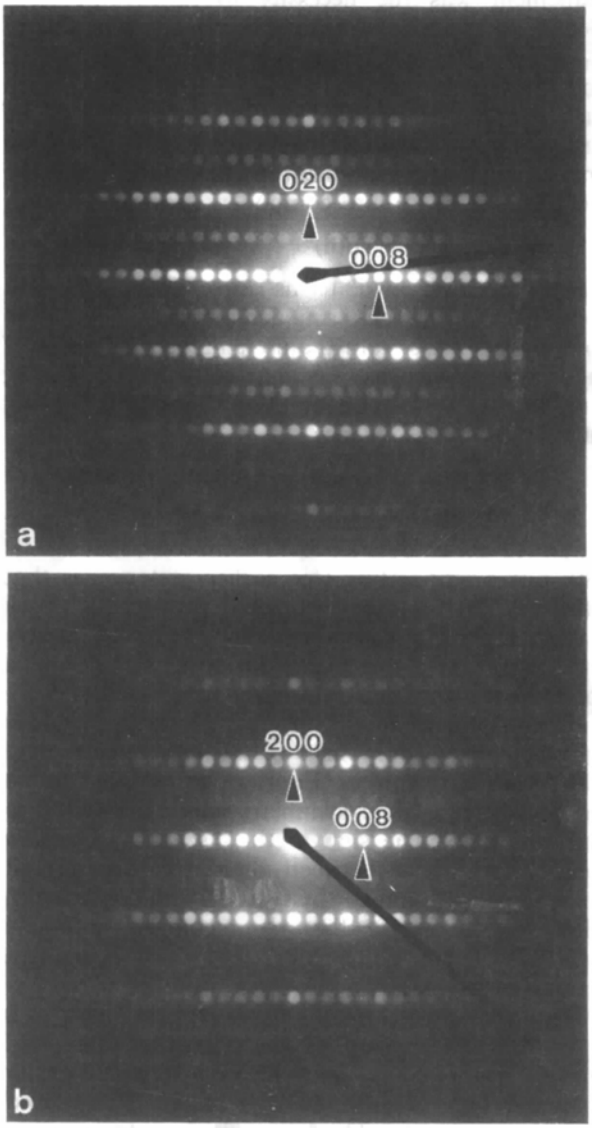

Fig. 2. Typical [100] (*a*), [010] (*b*) and [001] (*c*) zone-axis convergent-beam patterns (CBP's). The three patterns taken together, require a space-group symmetry of at least $A1a1$ and are certainly compatible with $A2_1am$ space-group symmetry.

does all information about the relative signs of symmetrized components of the scattering density.

Structures are usually described in terms of atom-based parameters and in principle the correct structure should best fit the data. However, the distinction in refinement statistics between correct and incorrect stable answers may be quite small as evidenced in other Aurivillius phases we have studied. A description of $F(\mathbf{h})$ for a modulated structure as a Taylor expansion about the value $F(\mathbf{h})_0$ of an idealized parent structure of *Fmmm* symmetry defines the nature of the problem (Rae *et al.*, 1991). If the expansion is truncated after the first-order terms, then, in the absence of anomalous dispersion, there is no difference in calculated intensity should the sign of all the symmetrized parameter combinations describing a particular component, *Amam* say, be reversed. Correlations that distinguish relative signs of the displacive modes occur in the second- and higher-order terms of the expansion, but if displacements are small then the differences in intensity are small.

It should be noted that the second-order terms can be compensated for by changes in anisotropic thermal parameters. Least-squares refinement implicitly assumes that phases calculated from a model are correct but in modulated structures there is no guarantee that the refinement will correct mistakes in the signs chosen for atom displacements away from their positions in the parent structure. Comparative refinement is essential, *i.e.* the refinement of alternative starting models must be compared and it is quickly established that certain sign errors are self correcting and others are not, whether or not anomalous dispersion is present. Allowing anisotropic thermal parameters to take on physically unreasonable values is an important intermediate step in displacement-parameter self correction and is a diagnostic when self correction is attempted but not completed, resulting in an amplitude which is less than the correct value and a phase that is still wrong. For large displacements the barrier to self correction is also large because certain symmetrized components of the scattering density (*e.g.* the *Fmmm* component of a structure of $A2_1am$ symmetry) do not distinguish between the correct and incorrect sign of a displacive modulation and in these circumstances anisotropic thermal parameters appear to be reasonable since the displacive amplitude is close to the correct value.

A further problem is that unrecognized disorder can result in diminished amplitudes for some modes, *e.g.* the *F2mm* and *Abam* modes of *Fmmm* being modulated to $A2_1am$. From equation (2) the erroneous modelling of $(1 - 2a)B(\mathbf{h})$ as $B(\mathbf{h})$ for *F*-centred data results in the *F2mm* mode being reduced in amplitude by $(1 - 2a)$. In the absence of anomalous dispersion, the distinction between these two models is only evident in the second- and higher-order terms of the Taylor expansion and the second-order terms can be compensated for by changes in anisotropic thermal parameters. There is an associated increase in apparent thermal motion in the direction of atom displacements that contribute to $B(\mathbf{h})$. A similar result applies to the *Abam* mode.

The presence of anomalous dispersion has very definite benefits. The contribution to the structure factors from the *Fmmm* and *Abam* symmetrized components of the scattering density is now $A(\mathbf{h}) + iA''(\mathbf{h})$ rather than $A(\mathbf{h})$ while the contribution from the *F2mm* and *Amam* components is $iB(\mathbf{h}) - B''(\mathbf{h})$ rather than $iB(\mathbf{h})$ so that there are now correlations between the phases of different symmetrized components, *i.e.* $k_1[A''(\mathbf{h})B(\mathbf{h}) - B''(\mathbf{h})A(\mathbf{h})]$ changes sign if either $A(\mathbf{h})$ or $B(\mathbf{h})$ changes sign. This enhances the difference between agreement factors for comparative refinement.

If a disorder-only model is used then it is seen that the values of k_1 and k_2 are incompatible should disorder and twinning both exist. If a twinned but not disordered model is used a reasonably good fit is obtained by reducing the amplitude of the *F2mm* and *Abam* modes by $(1 - 2a)$ as before, only now the contribution of the final term in equation (2) [either $B''(\mathbf{h})^2$ or $A''(\mathbf{h})^2$] is incorrectly scaled. In the present structure the *F*-centered data have a large contribution to $B''(\mathbf{h})$ data from the Bi atom having a substantial *F2mm* displacement along **a**. (The disordering plane defines the origin in the **a** direction.) The correct scaling of the $B''(\mathbf{h})$ contribution by including disorder reduces the minimum obtainable value of R_1 from 0.058 to 0.045 with R_1 for the *eee* data reducing from 0.062 to 0.043.

A further feature of the correlation term is that it allows refinement to be initiated from a starting model in which the amplitudes of the *F2mm* and *Abam* displacements are zero. In the latter case the *Amam* displacement must be non-zero. This is not possible in the absence of anomalous dispersion. The success of this ploy depends on either $A''(\mathbf{h})$ being large or $B''(\mathbf{h})$ being large. The $iA''(\mathbf{h})$ is necessarily large for the *Fmmm* component as it is associated with the parent structure that contains Bi and Ta and so the *F2mm* component of $F(\mathbf{h})$ can be refined from zero displacement, so defining the direction of polarization. For *A*-centred data it is fortuitous that there is a substantial y displacement of the anomalous-scatterer Bi that makes a substantial contribution to the *Amam* component, allowing it to dominate the data so that the *Abam* component can be refined from an initial model containing zero amplitude for this displacive mode.

The success of refinement of symmetrized components depends on phase reliability for the

associated components of the structure factors and strategies comparable to heavy-atom refinements are required. The first step is to identify the major contributor to a class of reflections. Here, apart from the parent-structure symmetry component, size is determined by the product of scattering factor and symmetrized displacement from the parent-structure position. Smaller-size contributions can only be refined after larger contributions have been previously refined. The success of a zero-displacement starting model, see above, depends upon the anomalous scattering of another appropriate component being substantial and already modelled. The refinement of the *A*-centred data can be initiated by an arbitrary y displacement of the Bi atom, the relative sign selecting between origins, followed by refinement of the *Amam* mode alone, followed by refinement of the *Amam* and *Abam* modes together.

The refinement of weaker features of the displacive modes is very much influenced by correcting global parameters such as disorder, twinning and anisotropic extinction. Although it would be preferrable to have an ordered untwinned crystal, the nature of the structure makes this rather difficult to achieve. It has been shown that with appropriate parameterization the essential chemical features of the structure can still be obtained.

The refinement gave a value of 0.867 (4) for the occupancy parameter a, 0.35 (2) for the twin parameter b and 0.032 (2) for the twin parameter c. This implies the intensities of the *A*-centered data were reduced by 6.4% relative to the *F*-centered data. This was in agreement with diffractometry evidence of reflections in the *B*-centered positions of the reciprocal lattice. The twin ratio of the first two components is 0.63:0.37 and this gives values of -0.38 (6) and 0.54 (1) for k_1 and k_2 respectively in equation (1). An untwinned non-disordered structure would have had values of ± 2 and 1 respectively. The small value of k_1 reduces the difference between Friedel-related reflections by the factor $k_1/2$. This is evidenced in the merge statistics.

Structure refinement of $Bi_2SrTa_2O_9$

Initial refinement of $Bi_2SrTa_2O_9$ in space group $A2_1am$ used a model which did not include either twinning or disorder and the refinement was not really any better than that of previous workers (Newnham *et al.*, 1973). Using a twinned but not disordered model it was possible to reduce the value of R_1 from above 0.10 to 0.058 for the observed data. This refinement used the twinning parameters b and c described earlier. Up to this stage the origin along **a** was chosen by fixing the x coordinate of the Bi atom. The polar direction was chosen by initial refinement of the Sr and Ta atoms away from their *Fmmm* parent-structure positions and was shown to be correct by comparative refinement. The refinement of the *A*-centred data was initiated by constraining the *Abam* mode to have zero amplitude and giving the y coordinate of the Bi atom an arbitrary displacement to initiate refinement of the *Amam* mode. (Such a strategy would have been inappropriate for a neutron diffraction study.) Subsequently all atoms were allowed to refine using anisotropic thermal parameters for all atoms and initiating refinement of the O atoms from their parent-structure positions. Equivalent reflections were not merged and anisotropic extinction corrections were applied. The type-2 parameterization of Coppens & Hamilton (1970) was used. Final values of $W'_{11} = 16$ (2), $W'_{22} = 3.6$ (9), $W'_{33} = 240$ (40), $W'_{12} = -3.9$ (7), $W'_{13} = 41$ (6), $W'_{23} = 6$ (5) were obtained. The refinement gave small thermal parameters for the Sr and Ta atoms but a large thermal parameter of $U_{11} = 0.053$ (1) for displacement in the **a** direction.

A difference map was consistent with partial disorder across a plane perpendicular to **a** and passing approximately through the Ta atom. The minor component of the disorder had symmetrized coordinates for the heavy atoms directly comparable in phase, if not magnitude, with those for Bi_3TiNbO_9 (Thompson *et al.*, 1991). The components of the disorder have exactly the same symmetrized coordinates for the *Amam* mode but the signs for the symmetrized coordinates are reversed for the *F*2*mm* and *Abam* modes. The constrained least-squares refinement program *RAELS*89 was used to impose exact mirror symmetry to relate positional and anisotropic thermal parameters between the disordered halves, while adding a single occupancy parameter a (see earlier). The disorder causes partial overlap for all atom sites and it was considered realistic to refine only U_{ii} values for all but the Bi and Ta where all six U_{ij} values were refined for each atom. The sites of oxygen atoms O(4) overlap with the sites of oxygen atoms O(5) because of the disorder, and to control the amplitude of the very small *Abam* mode it was decided to set the thermal parameters of O(4) and O(5) equal and to have $U_{11} = U_{22}$ for these atoms. Refinement converged to give refinement statistics effectively the same as those for the final structure listed in Table 3. However certain features of the refinement did not appear satisfactory.

Identification of a false minimum in the refinement

The parameters adopted for the atomic coordinates of atoms O(4) and O(5) did not appear satisfactory when broken down into symmetrized-parameter combinations and it was realized that the y coordinate of atom O(4) could be on the wrong side of $y = 0.25$. This coordinate for O(4) was changed to

$0.5 - y$ and refinement recommenced. An extremely marginal improvement in goodness of fit and R_1 resulted for both *A*- and *F*-centered data but the overall improvement in R_1 was only from 0.0449 to 0.0448 for the observed data. Both refinements were stable but the second solution made more chemical sense, resulting in less distortion of the TaO_6 octahedron. The refined coordinates of atoms O(4) and O(5) before and after the switch of y coordinate on O(4) were as follows:

	False minimum			Correct minimum		
O(4)	0.2463 (26)	0.2367 (25)	0.5697 (3)	0.2414 (25)	0.2556 (19)	0.5697 (3)
O(5)	0.2650 (22)	−0.2282 (19)	0.5830 (3)	0.2625 (22)	0.2325 (15)	0.5831 (3)

When broken into normal modes the contributions to O(4) become:

	False minimum			Correct minimum		
Fmmm	0.25	0.25	0.5764	0.25	0.25	0.5764
F2mm	0.0056	0.0175	0.0	0.0019	0.0055	0.0
Amam	0.0	0.0	0.0067	0.0	0.0	−0.0067
Abam	0.0094	0.0044	0.0	0.0105	0.0100	0.0

The contributions to O(5) have the same magnitudes but signs as detailed in Table 4.

The phenomenom is understood when it is realized that those terms in the Taylor series expansion that should be investigated to analyse the refinement of these atoms are the first- and second-order terms that contribute to the *Fmmm* and *Amam* components of the structure factors. The first-order contributions of the *F2mm* and *Abam* modes are of lesser importance but in combination with the other considerations they do discriminate slightly in favour of the preferred solution. It is noted that the signs of these first-order contributions are unchanged but the uncertainty in magnitudes causes the problem since reflection amplitudes are dominated by the *Fmmm* and *Amam* components. The false minimum is associated with the history of the refinement. A refinement cycle constrained so that the *Abam* component was exactly zero preceded a refinement in which this component was allowed to refine away from zero amplitude. The initial refinement made the y coordinate in question less than 0.25 and the subsequent refinement was incapable of making y greater than 0.25. It is seen in the preferred solution that the *F2mm* displacements are diminished while the *Abam* displacements are increased. The amplitude for the *F2mm* mode for these atoms was even larger when the amplitude of the *Abam* mode was fixed at zero.

Because of the symmetry products *F2mm*F2mm* = *Fmmm* and *Abam*Abam* = *Fmmm* (see Rae *et al.*, 1991) we create $\sum_{i=1,2}\Delta x_i\Delta x_i$, $\sum_i\Delta y_i\Delta y_i$ and $2\sum_i\Delta x_i\Delta y_i$ contributions of *Fmmm* symmetry in the Taylor expansion with values of 120, 324 and −280 (all $\times 10^{-6}$) respectively for the false minimum and 114, 130 and −231 (all $\times 10^{-6}$) for the preferred option. The difference in anisotropic vibration parameters, particularly U_{22}, accounts for the difference. The symmetry products *F2mm*Abam* = *Abam*F2mm* = *Amam* create contributions of *Amam* symmetry and the signs of the second-order terms are again in agreement. The signs for these second-order contributions swap between *F*- and *A*-centred data reducing correlation with thermal parameters. The consequences of the inconsistency between amplitudes of these terms is diminished because of the dominance of the more reliably observed *F*-centred data in the refinement. It is the compensating nature of the parameter changes to maintain the integrity of the *Fmmm* component of the structure factor that stabilizes the false minimum.

Structure description and crystal chemistry

Final atomic coordinates are listed in Table 1.* Positions for disorder-related atoms are obtained by changing x, y, z values to $-x$, y, z. Final thermal parameters are listed in Table 2. Parameters for disorder-related atoms are the same except that U_{12} and U_{13} change sign. It should be noted that thermal parameters for the comparable structure Bi_3TiNbO_9 (Thompson *et al.*, 1991) have inadvertantly been described as ($\times 10^{-3}$ Å^2) rather than ($\times$ Å^2). Final refinement statistics are given in Table 3. Table 4 contains a resolution of atomic parameters into the displacive modes of different symmetry. These displacive modes have been illustrated schematically previously (Thompson *et al.*, 1991). The earlier refinement of $(Sr_{0.9}Ba_{0.1})Bi_2Ta_2O_9$ as well as the closely related Bi_3TiNbO_9 are also presented in this way for comparison. The origin along **a** has been chosen to coincide with the Bi at the perovskite *B* site in order to describe the *F2mm* mode. Table 5 gives the geometry of the Sr, Bi and Ta environments in $Bi_2SrTa_2O_9$.

Comparison of the signs and magnitudes of the various displacive modes between the present $Bi_2SrTa_2O_9$ and the earlier $(Sr_{0.9}Ba_{0.1})Bi_2Ta_2O_9$ refinements shows the *Abam* and *Amam* modes to be in reasonable agreement. In general the displacements for these two modes are smaller in the present work. The major disagreement occurs in the *F2mm* mode. Most strikingly different are the Δx shifts on O(1) and O(2), the former being three times larger than and the latter of opposite sign to the present work.

A comparison between $Bi_2SrTa_2O_9$ and Bi_3TiNbO_9, however, shows some very interesting

* Lists of structure factors have been deposited with the British Library Document Supply Centre as Supplementary Publication No. SUP 54994 (24 pp.). Copies may be obtained through The Technical Editor, International Union of Crystallography, 5 Abbey Square, Chester CH1 2HU, England. [CIF reference: AL0520]

Table 1. *Positional parameters of* $Bi_2SrTa_2O_9$

Parameters for the second disorder component are obtained by changing x to $-x$.

	x	y	z
Sr	−0.0220 (11)	0.5054 (2)	0.5000 (−)
Bi	−0.0486 (8)	0.4732 (1)	0.7007 (0)
Ta	−0.0137 (12)	0.0022 (1)	0.5849 (0)
O(1)	−0.0131 (39)	−0.0428 (17)	0.5000 (−)
O(2)	−0.0071 (32)	0.0555 (14)	0.6591 (3)
O(3)	0.2183 (23)	0.2407 (45)	0.2492 (2)
O(4)	0.2414 (25)	0.2556 (19)	0.5697 (3)
O(5)	0.2625 (22)	−0.2335 (15)	0.5831 (3)

Table 2. *U_{ij} thermal parameters for* $Bi_2SrTa_2O_9$ (Å^2)

	U_{11}	U_{22}	U_{33}	U_{12}	U_{13}	U_{23}	$\langle U \rangle$
Sr	0.001 (1)	0.003 (1)	0.001 (1)	0.000 ( )	0.000 (−)	0.000 ( )	0.002 (0)
Bi	0.029 (1)	0.018 (0)	0.012 (0)	0.001 (0)	0.005 (0)	0.003 (0)	0.019 (0)
Ta	−0.001 (0)	0.000 (0)	0.004 (0)	0.000 (0)	0.000 (0)	0.000 (0)	0.001 (0)
O(1)	0.018 (7)	0.006 (3)	0.016 (6)	0.000 (−)	0.000 (−)	0.000 ( )	0.013 (2)
O(2)	0.031 (6)	0.021 (3)	−0.001 (3)	0.000 ( )	0.000 ( )	0.000 (−)	0.017 (2)
O(3)	0.011 (7)	−0.001 (3)	−0.002 (3)	0.000 (−)	0.000 (−)	0.000 ( )	0.003 (2)
O(4)	0.006 (1)	0.006 (1)	0.005 (3)	0.000 (−)	0.000 (−)	0.000 ( )	0.006 (1)
O(5)	0.006 (1)	0.006 (1)	0.005 (3)	0.000 ( )	0.000 (−)	0.000 (−)	0.006 (1)

Table 3. *Final refinement statistics for* $Bi_2SrTa_2O_9$

Data set	R_1	wR	G.o.f.
All 3083 observed data	0.0448	0.0715	1.96
(1) 924 *eee* data	0.0429	0.0808	2.45
(2) 941 *ooo* data	0.0415	0.0631	1.92
(3) 647 *eoo* data	0.0570	0.0709	1.55
(4) 571 *oee* data	0.0568	0.0670	1.52
(5) 16 ($\sin\theta/\lambda < 0.1$ Å^{-1}) data	0.1070	0.1542	4.09
(6) 49 ($0.1 < \sin\theta/\lambda < 0.2$ Å^{-1}) data	0.0747	0.2034	6.14
(7)* 457 [$I < 3\sigma(I)$] data	0.4218	0.3273	1.11

Notes: $R_1 = \sum_{\mathbf{h}} |F_{obs}(\mathbf{h}) - |F_{calc}(\mathbf{h})| / \sum_{\mathbf{h}} |F_{obs}(\mathbf{h})|$,
$wR = [\sum_{\mathbf{h}} w_{\mathbf{h}} (|F_{obs}(\mathbf{h})| - |F_{calc}(\mathbf{h})|)^2 / \sum_{\mathbf{h}} w_{\mathbf{h}} |F_{obs}(\mathbf{h})|^2]^{1/2}$,
G.o.f. $= [\sum_{\mathbf{h}} w_{\mathbf{h}} (|F_{obs}(\mathbf{h})| - |F_{calc}(\mathbf{h})|)^2 / (n - m)]^{1/2}$.

* Data omitted during refinement.

similarities and contrasts. The *Amam* mode is similar both in sign and magnitude corresponding to an octahedral rotation about **a** of 7.3° in $Bi_2SrTa_2O_9$ compared with 8.9° in Bi_3TiNbO_9 [see Fig. 3 of Withers *et al.* (1991)]. Neither the magnitude nor the sign are dependent on whether or not disorder and twinning are included in the refined model. The mode is unchanged across the twin/disorder boundaries of the centrosymmetrically related domains. Only the Δy component on the Sr and O(1) atoms shows a significant difference for the *Amam* mode and this corresponds to an approximate halving in amplitude relative to the corresponding atoms in Bi_3TiNbO_9 and does contribute to the above-mentioned small reduction in the octahedral rotation about **a**. In contrast the *Abam* mode is strikingly different and in terms of rotation of the MO_6 octahedron about **c** equates to an angle of only 2.4° compared with 9.1° in Bi_3TiNbO_9 [see Fig. 4 of Withers *et al.* (1991)]. The *F2mm* mode is similar in magnitude and sign for most atoms except again for Sr and O(1). The Δx shift for Sr changes both sign

Table 4. *Amplitudes of displacive modes for* $Bi_2SrTa_2O_9$, *present and earlier refinement, compared with* Bi_3TiNbO_9

Displacements are given as fractions of unit-cell dimensions ($\times 10^4$).

		F2mm		*Amam*		*Abam*	
	Structure	Δx	Δy	Δy	Δz	Δx	Δy
Sr(1)	Rae	266	0	54	0	0	0
	Newnham	200	0	70	0	0	0
Bi(1)	Thompson	−59	0	100	0	0	0
	Rae	0*	0	−268	0	0	0
	Newnham	0*	0	−220	0	0	0
Bi(2)	Thompson	0*	0	−199	0	0	0
Ta(1)	Rae	349	0	22	0	0	0
	Newnham	360	0	30	0	0	0
Ti,Nb	Thompson	388	0	1	0	0	0
O(1)	Rae	355	0	−428	0	0	0
	Newnham	1020	0	−590	0	0	0
	Thompson	754	0	714	0	0	0
O(2)	Rae	415	0	555	0	0	0
	Newnham	−430	0	740	0	0	0
	Thompson	479	0	549	0	0	0
O(3)	Rae	169	0	0	−8	0	−93
	Newnham	280	0	0	−20	0	−170
	Thompson	129	0	0	−4	0	124
O(4)	Rae	506	−56	0	−67	−106	110
	Newnham	535	−45	0	−65	−205	165
	Thompson	645	−88	0	−77	−400	405
O(5)	Rae	506	56	0	67	106	110
	Newnham	535	45	0	65	205	165
	Thompson	645	88	0	77	400	405

* Constrained to be 0.0.

Table 5. *Geometry of the* Sr, Bi *and* Ta *environments in* Bi_2SrTaO_9

Distances (Å).
Only distances < 3.6 Å are listed. Distances in the same row of the table would be equivalent in the *Fmmm* parent structure. O atoms are coded to indicate which special position of *Fmmm* they have been displaced from, *viz.* (*a*) 0, 1, *z*; (*b*) $-\frac{1}{2}, \frac{1}{2}, z$; (*c*) 0, 0, *z*; (*d*) $\frac{1}{2}, \frac{1}{2}, z$; (*e*) $-\frac{1}{4}, \frac{3}{4}, -z+1$; (*f*) $-\frac{1}{4}, \frac{3}{4}, z$; (*g*) $\frac{1}{4}, \frac{3}{4}, z$; (*h*) $\frac{1}{4}, \frac{3}{4}, 1-z$; (*i*) $\frac{1}{4}, \frac{1}{4}, z$; (*j*) $\frac{1}{4}, \frac{1}{4}, -z+1$; (*k*) $-\frac{1}{4}, \frac{1}{4}, -z+1$; (*l*) $-\frac{1}{4}, \frac{1}{4}, z$; (*m*) 0, $\frac{1}{2}$, $-z+\frac{3}{2}$; (*n*) $-\frac{1}{4}, -\frac{1}{4}, z$; (*o*) $\frac{1}{4}, -\frac{1}{4}, z$.

Sr—O(1)*a*	2.501 (9)	—O(1)*b*	2.724 (21)	—O(1)*d*	2.822 (21)	—O(1)*c* 3.034 (9)
—O(4)*k*	2.614 (11)	—O(4)*l*	2.614 (11)	—O(4)*i*	2.658 (11)	—O(4)*j* 2.658 (9)
—O(5)*e*	2.707 (7)	—O(5)*f*	2.707 (7)	—O(5)*g*	2.979 (8)	—O(5)*h* 2.979 (8)
Bi—O(2)*c*	2.545 (8)	—O(2)*b*	2.745 (16)	—O(2)*d*	3.175 (16)	—O(2)*a* 3.394 (8)
—O(3)*k*	2.151 (16)	—O(3)*j*	2.324 (16)	—O(3)*e*	2.374 (11)	—O(3)*h* 2.416 (12)
—O(5)*f*	3.435 (7)					
—O(2)*m*	3.540 (8)					
Ta—O(4)*l*	1.943 (10)	—O(4)*i*	2.026 (10)	—O(5)*n*	1.935 (11)	—O(5)*o* 2.009 (11)
—O(1)*c*	2.136 (1)	—O(2)*c*	1.876 (8)			

O—Ta—O angles (°)

O(1)*c*	O(2)*c*	177.3 (5)	O(1)*c*	O(4)*l*	83.5 (5)	O(1)*c*	O(4)*i*	83.9 (4)
O(1)*c*	O(5)*o*	84.3 (5)	O(1)*c*	O(5)*n*	83.6 (4)	O(2)*c*	O(4)*l*	95.6 (4)
O(2)*c*	O(4)*i*	92.6 (5)	O(2)*c*	O(5)*o*	96.3 (4)	O(2)*c*	O(5)*n*	99.0 (4)
O(4)*i*	O(4)*l*	88.3 (1)	O(4)*i*	O(5)*o*	85.2 (5)	O(4)*l*	O(5)*o*	166.8 (3)
O(4)*l*	O(5)*n*	94.6 (5)	O(4)*i*	O(5)*n*	166.7 (3)	O(5)*o*	O(5)*n*	89.3 (1)

and magnitude while the magnitude for O(1) is halved. A better picture is in terms of differences in x displacements within this mode. The difference for Sr minus O(1) is −0.0089 compared to −0.0813 for Bi(1) minus O(1) in Bi_3TiNbO_9, a very substantial reduction. The difference in x coordinates for O(1) minus O(2) is −0.0060 compared to 0.0275 for Bi_3TiNbO_9. These atoms are opposite each other in the octahedron of O atoms surrounding the Ta. The

result shows that in $Bi_2SrTa_2O_9$ the TaO_6 coordination octahedra are much more aligned with the **c** axis and the polarity can be quite well described as a movement of the Ta, O(4) and O(5) relative to Bi(1) and O(3) of the Bi_2O_2 layer with an additional movement of Ta relative to O(4) and O(5). This coincides with the propensity for twinning and disorder in these crystals with layers of TaO_6 octahedra on either side of the Bi_2O_2 losing coherence. The very similar axial lengths for *a* and *b* assist the creation of {110} twins.

We have calculated apparent valences (AV's) for $Bi_2SrTa_2O_9$ using r_0's listed in Brown & Altermatt (1985) for both the parent and final refined structures as well as mode by mode. These are listed in Table 6. As discussed earlier the parent structure of $Bi_2SrTa_2O_9$ is different from the parent structures of $Bi_4Ti_3O_{12}$, Bi_3TiNbO_9 and Bi_2WO_6 in that the perovskite *A*-atom site is occupied by a divalent cation which is already overbonded. Any distortion away from this high-symmetry parent structure will only cause further overbonding. At the same time the Bi atom in the Bi_2O_2 layer is underbonded and the Ta in the TaO_6 octahedron slightly overbonded, both seeking to achieve a more satisfactory bonding environment by appropriate distortion from the parent structure. The underbonding of Bi(2) in Bi_3TiNbO_9 was relieved by a combination of the *F2mm* and *Amam* modes. The overbonding of Ti,Nb was relieved by a combination of the *Amam* and *Abam* modes. In $Bi_2SrTa_2O_9$ the *F2mm* and *Amam* modes are together able to relieve the underbonding of Bi but, as outlined above, these modes appear to be suppressed in the vicinity of the perovskite *A* atom. This is reflected in the *Amam* Δy shifts and the *F2mm* Δx shifts of the Sr and O(1) atoms. The *Abam* mode, which serves to relieve the overbonding of Ti,Nb and the underbonding of Bi(2) in Bi_3TiNbO_9, is almost non-existent in $Bi_2SrTa_2O_9$ and has little effect on the AV's (see column headed '*Abam*' in Table 6).

These differences between $Bi_2SrTa_2O_9$ and Bi_3TiNbO_9 clearly arise from the difference in the perovskite *A* atom in the respective structures. It appears that, unlike Bi_3TiNbO_9 which manages to satisfy the bonding requirements of most atoms, $Bi_2SrTa_2O_9$ is slightly frustrated by its inability to simultaneously relieve the overbonding of Ta and the underbonding of Bi while preserving as far as possible the high-symmetry 12-coordinate Sr site. Unlike Bi(1) in Bi_3TiNbO_9, Sr retains a fairly regular 12-coordinate site as reflected in the narrow distribution of Sr—O bond lengths (see Table 5). The frustration is evident in the residual underbonding of Bi and overbonding of Ta in $Bi_2SrTa_2O_9$.

From the present work a value for P_s of 14.4 $\mu C\,cm^{-2}$ is calculated for an untwinned non-

Table 6. *Apparent valences for* $Bi_2SrTa_2O_9$

	Parent	*F2mm*	*Amam*	*Abam*	2 modes*	Total†	Newnham‡
Sr§	2.21	2.24	2.34	2.23	2.37	2.37	2.76
Bi	2.69	2.74	2.86	2.70	2.90	2.91	3.11
Ta	5.29	5.30	5.13	5.28	5.13	5.12	5.18
O(1)	1.86	1.86	1.90	1.86	1.90	1.90	2.12
O(2)	1.61	1.64	1.67	1.61	1.69	1.69	1.72
O(3)	2.22	2.24	2.25	2.22	2.27	2.28	2.46
O(4)	2.17	2.18	2.20	2.16	2.21	2.21	2.28
O(5)	2.17	2.18	2.09	2.16	2.10	2.08	2.14

* The sum of the *F2mm* and *Amam* displacements.
† The sum of all three modes, the final refined structure.
‡ The refined structure of Newnham *et al.* (1973) using r_0 $(Ba_{0.1}Sr_{0.9})$—O = 2.135.
§ $(Ba_{0.1}Sr_{0.9})$ for the Newnham *et al.* (1973) structure.

disordered crystal of $Bi_2SrTa_2O_9$. While this is not in good agreement with the estimated value for P_s of 5.8 $\mu C\,cm^{-2}$ (Subbarao, 1962) this experimental value cannot be given much weight given that it was determined indirectly from a polycrystalline specimen. Of more importance is the experimental work of Newnham *et al.* (1973) on $(Sr_{0.9}Ba_{0.1})Bi_2Ta_2O_9$. They chose that composition to bring the phase transitions closer to room temperature as $Bi_2SrTa_2O_9$ has phase transitions at 583 and 843 K, while $Bi_2BaTa_2O_9$ shows no transitions to 77 K. For their chosen composition Newnham *et al.* (1973) observed phase transitions at ~483 and ~523 K and measured a P_s of ~8 $\mu C\,cm^{-2}$ using a single crystal. That the calculated P_s for $Bi_2SrTa_2O_9$ is somewhat larger than that observed for $(Sr_{0.9}Ba_{0.1})Bi_2Ta_2O_9$ is consistent with the T_c–P_s relationship for the Aurivillius phases described by Singh, Bopardikar & Atkare (1988). On the other hand we note that the P_s for $Bi_2SrTa_2O_9$ is only half that of Bi_3TiNbO_9, namely 27.7 $\mu C\,cm^{-2}$. This too is consistent with the same T_c–P_s relationship mentioned above as Bi_3TiNbO_9 has transitions at 1023 and 1213 K. The difference in the calculated P_s between $Bi_2SrTa_2O_9$ and Bi_3TiNbO_9 is readily identified in the Δx shift of the perovskite *A* atom and O(1) in the ferroelectric *F2mm* displacive mode (see Table 4).

The reduction of T_c and the associated lowering of P_s by the substitution of Ba for Sr in $Bi_2SrTa_2O_9$ can also be understood in bond-valence terms. We have already noted that Sr is overbonded in the undistorted parent structure. It follows that substituting Ba for Sr will only serve to increase the overbonding as the R_0 for Ba—O is 2.285 compared with R_0 for Sr—O of 2.118. In the hypothetical $Bi_2BaTa_2O_9$ parent structure this would give an AV for Ba of 3.2. From the arguments given above for Sr in $Bi_2SrTa_2O_9$ concerning the suppression of the displacive modes by the overbonded perovskite *A* atom it would follow that these modes would be even more strongly suppressed in $Bi_2BaTa_2O_9$. Experimentally it appears that at room temperature these modes are suppressed completely.

The authors wish to thank Dr A. C. Willis for generous assistance with X-ray data collection.

References

ALCOCK, N. W. (1970). *Acta Cryst.* A**26**, 437–439.

BROWN, I. D. (1978). *Chem. Soc. Rev.* **7**, 359–376.

BROWN, I. D. (1981). *Structure and Bonding in Crystals*, Vol. 2, edited by M. O'KEEFFE & A. NAVROTSKY, pp. 1–30. New York: Academic Press.

BROWN, I. D. & ALTERMATT, D. (1985). *Acta Cryst.* B**41**, 244–247.

COPPENS, P. & HAMILTON, W. C. (1970). *Acta Cryst.* A**26**, 71–83.

DORRIAN, J. F., NEWNHAM, R. E., SMITH, T. K. & KAY, M. I. (1971). *Ferroelectrics*, **3**, 17–27.

HALL, S. R. & STEWART, J. M. (1990). Editors. *XTAL3.0 Users Manual*. Univs. of Western Australia, Australia, and Maryland, USA.

NEWNHAM, R. E., WOLFE, R. W., HORSEY, R. S., DIAZ-COLON, F. A. & KAY, M. I. (1973). *Mater. Res. Bull.* **8**, 1183–1195.

RAE, A. D. (1989). *RAELS89. A Comprehensive Constrined Least-Squares Refinement Program*. Univ. of New South Wales, Australia.

RAE, A. D., THOMPSON, J. G. & WITHERS, R. L. (1991). *Acta Cryst.* B**47**, 870–881.

RAE, A. D., THOMPSON, J. G., WITHERS, R. L. & WILLIS, A. C. (1990). *Acta Cryst.* B**46**, 474–487.

SHELDRICK, G. M. (1976). *SHELX76*. Program for crystal structure determination. Univ. of Cambridge, England.

SINGH, K., BOPARDIKAR, D. K. & ATKARE, D. V. (1988). *Ferroelectrics*, **82**, 55–67.

SUBBARAO, E. C. (1962). *J. Phys. Chem. Solids*, **23**, 665–676.

THOMPSON, J. G., RAE, A. D., WITHERS, R. L. & CRAIG, D. C. (1991). *Acta Cryst.* B**47**, 174–180.

WITHERS, R. L., THOMPSON, J. G. & RAE, A. D. (1991). *J. Solid State Chem.* **94**, 404–417.

WOLFE, R. W., NEWNHAM, R. E. & KAY, M. I. (1969). *Solid State Commun.* **7**, 1797–1801.

WOLFE, R. W., NEWNHAM, R. E., SMITH, T. K. & KAY, M. I. (1971). *Ferroelectrics*, **3**, 1–7.

Acta Cryst. (1992). B**48**, 428–437

Structure of $(\eta^6\text{-}C_6H_6)Mo(CO)_3$ at Room Temperature and 120 K: Motion about Equilibrium and Far from Equilibrium

BY HANS-BEAT BÜRGI AND ANDREA RASELLI

Laboratory for Chemical and Mineralogical Crystallography, University of Bern, CH-3012, Switzerland

AND DARIO BRAGA AND FABRIZIA GREPIONI

Dipartimento di Chimica 'G. Ciamician', Università di Bologna, Via F. Selmi 2, 40126 *Bologna, Italy*

(*Received* 28 *September* 1991; *accepted* 3 *December* 1991)

Abstract

The structure of (η^6-benzene)tricarbonylmolybdenum, $(\eta^6\text{-}C_6H_6)Mo(CO)_3$, has been determined at room temperature and 120 K by single-crystal X-ray diffractometry. The molecular motion about equilibrium has been studied by means of thermal-motion analysis, showing that there is significant stretching motion of C_6H_6 and CO relative to Mo. There are effects of molecular packing on the motion of the CO's and on the deviation of the molecular structure from C_{3v} symmetry which are mutually consistent. The motional features and the deviations from symmetry are very similar to those of the isostructural $(\eta^6\text{-}C_6H_6)Cr(CO)_3$. The reorientational motion of the C_6H_6 group has been explored by potential-energy-barrier calculations within the atom–atom approach. The results are compared with the available solid-state spectroscopic information. $(\eta^6\text{-}C_6H_6)Mo(CO)_3$ is monoclinic at room temperature [$a = 6.162$ (3), $b = 11.096$ (2), $c = 6.826$ (2) Å, $\beta = 101.64$ (3)°, $V = 457.12$ Å^3], and at 120 K [$a = 6.028$ (1), $b = 11.001$ (2), $c = 6.763$ (1) Å, $\beta = 100.79$ (1)°, $V = 440.55$ Å^3], space group $P2_1/m$, $Z = 2$.

Introduction

$(\eta^6\text{-}C_6H_6)M(CO)_3$ (M = Cr, Mo) represents the prototype of a large family of $(\eta^6$-arene$)ML_3$ species (Muetterties, Bleeke, Wucherer & Albright, 1982). The solid-state structure of $(\eta^6\text{-}C_6H_6)Cr(CO)_3$ has been studied at room and at low temperature by both X-ray and neutron diffraction methods (Corradini & Allegra, 1959; Bailey & Dahl, 1965*b*; Rees & Coppens, 1973; Wang, Angermund, Goddard & Kruger, 1987). The low-temperature structural work has shown that the C—C bonds '*trans*' to the chromium–carbonyl ones are shorter than the others by *ca* 0.017 Å (Rees & Coppens, 1973; Wang *et al.*, 1987). This result was also substantiated by extended Hückel calculations (Albright, Hofmann & Hoffman, 1977; Kok & Hall, 1985). We now report an X-ray crystallographic characterization of the Mo analogue at room temperature and 120 K. The aims of the paper can be summarized as follows:

0108-7681/92/040428-10$06.00